IRANIAN JOURNAL OF PHYSICS RESEARCH

Iranian Journal of Physics Research, Vol. 16, No. 3, 2016

DC conductivity studies of ZnS and Ag nanoparticles doped P3HT thin films

T Abdul Kareem

Radiation Physics, University of Calicut, Malappuram, Kerala, India

(Received 14 April 2015 ; in final form 31 May 2016)

Abstract

Interest in the P3HT: ZnS nanocomposites are increased due to their applicability as an active layer for bulk heterojunction solar cells of high open circuit voltage and charge transport in this type of solar cells determines their performance. So the study of the conduction mechanism of the P3HT:ZnS nanocomposites is significant to improve the efficiency of such solar cells, and this paper discusses both the Arrhenius Model and the Variable Range Hopping (VRH) conduction mechanism in the P3HT:ZnS nanocomposite films. It is found that the addition of the semiconductor nanoparticles does not make any remarkable change in the room temperature DC conduction of P3HT polymer. Further, the films have been studied by their absorption spectra, x-ray diffractogram, scanning electron microscope and noncontact profilometer.

Keywords: P3HT:ZnS, DC conductivity, VRH conduction, Arrhenius model

1. Introduction

Bulk heterojunction solar cells made up of conducting polymers are presently the most studied solar cells, where the electron accepting nanoparticles are mixed with the electron donating polymer and the exciton created in the donor diffuses to the interface to enable the charge separation. Various combinations of donor and acceptor materials have been used to build bulk heterojunction solar cells, especially polymer – fullerene (polymer - PCBM) solar cells are the most studied combination bulk-heterojunction cells [1-5] and recently ZnS nanoparticles [6,7] also have been tested with P3HT polymer for bulk heterojunction solar cells.

Semiconducting ZnS is preferred as an electron acceptor with the donor P3HT, because it is environment friendly, stable indefinitely and can be synthesized easily and inexpensively. It is supposed that the LUMO level of the inorganic semiconductor is less at least 0.3 eV than that of P3HT [8], since the quantum confinement effect of the semiconducting nanocrystals shifts their LUMO level ~~to~~ upward and shifts HOMO downward, the band gap is enlarged [9]. The wide band of ZnS semiconductor has high electron mobility (600 $cm^2V^{-1}s^{-1}$ [10]) and has an electron affinity about 3.9eV [11]). This makes ZnS an attractive material to use as an electron acceptor in hybrid photovoltaic devices.

Charge transport in this nanocomposite determines the solar cell device performance, so that the study of the conduction mechanism of the P3HT:ZnS nanocomposites is significant to improve the efficiency of such bulk heterojunction solar cells. This paper discusses both the Arrhenius Model and the Variable Range Hopping (VRH) conduction mechanism in ZnS nanoparticles mixed with P3HT films. The significance of this study is that there is no literature available yet on these composites to compare their conduction properties.

2. Materials and methods

All chemicals were purchased from Sigma Aldrich Chemicals Ltd., Bangalore, while the sphalerite and wurtzite ZnS nanoparticles and poly vinyl alcohol coated silver nanoparticles [12] that are better for solar cells were prepared in the lab by simple wet chemical method using trisodium citrate and polyvinyl alcohol.

Four different samples of P3HT (20mg/ml in dichlorobenzene [13-17] were prepared for comparing device properties.

1) Pristine P3HT,

2) P3HT mixed with 1mg of ZnS_{cubic} nano particles

3) P3HT mixed with 1mg of ZnS_{Hexa} nano particles and 4) P3HT mixed with 1mg of ZnS_{Hexa} nano particles and 1mg PVA-Ag was prepared after comparing the solar cell performance of the above devices. It was found that the solar cell performance of P3HT:ZnS_{Hexa} was better

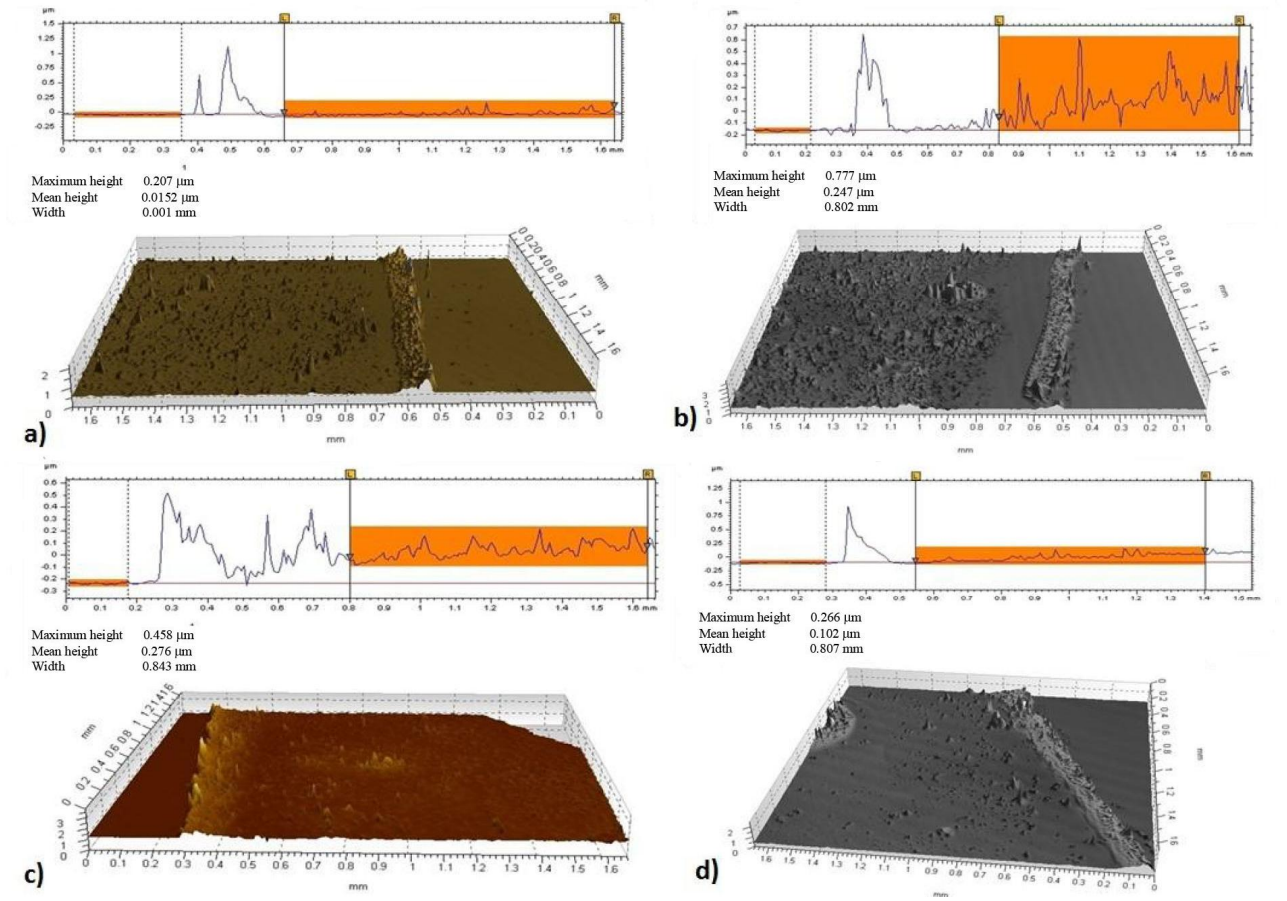

Figure 1. Surface images obtained from surface profilometer a)Glass/P3HT, b) Glass/P3HT:ZnSCubic, c) Glass/P3HT:ZnSHexa, d) Glass/P3HT:ZnSHexa:Ag-PVA.

Table 1. Thickness of the prepared thin films.

Sample Name	Thickness (nm)
Glass/P3HT	15.2
Glass/P3HT:ZnS_{Cubic}	247
Glass/P3HT:ZnS_{Hexa}	275
Glass/P3HT:ZnS_{Hexa}:Ag-PVA	102

than P3HT: ZnS_{cubic} and the results are not discussed here since the scope of the paper is to study the conduction properties. All samples were kept under stirring for 24 hour, then each drop of the samples was placed over the cleaned plane glass slides, where the spinner was spinning at 3000 rpm for 10 seconds in each case, and one edge of the plane glass slides was covered with cellophane tape to make 'step' for thickness measurement.

3. Results and discussion

Before any electrical measurements are taken, it is necessary to determine the thickness of the films whose characteristics are being measured, in order to be able to calculate or otherwise determine additional properties from the electrical or optical measurements. Here the thickness of the films coated over plane glass slides was found by Taylor Hobson Talysurf CCI MP interferometer (a non contact 3-D Profiler) and the scanned results are shown in figure 1. It is shown that the surface of the film is not smooth and average thickness of the films was found as given in table 1. It shows that the pristine P3HT film has lower thickness about 15.2 nm when comparing with other films it is found that the thickness varied with composition of the samples for the same rpm and this may be due to the change in the viscosity of the solution when ZnS and PVA-Ag was added.

Furthermore, the surface of the samples were probed by JEOL Model JSM - 6390LV SEM. SEM images of the samples including pristine P3HT, P3HT:ZnS_{Cubic}, P3HT:ZnS_{Hexa} and P3HT:ZnS_{Hexa}:PVA-Ag are shown in figure 2. These surface images confirm the surface results obtained from the profilometer observations that the surface is not smooth and the film is continuous without pinholes but ZnS particles are agglomerated over the surface of the films. The agglomerated ZnS particles of nanocrystallites over the surface have a positive impact on the device, the electron acceptor with nanoscale properties contacts with the bottom electrode, wavelength region and it may be due to the quantum confinement effect from the inorganic nano particles [7, 18, 20]. This blue shift of the absorption edge may be due to the rising in band gap between p and p* energy

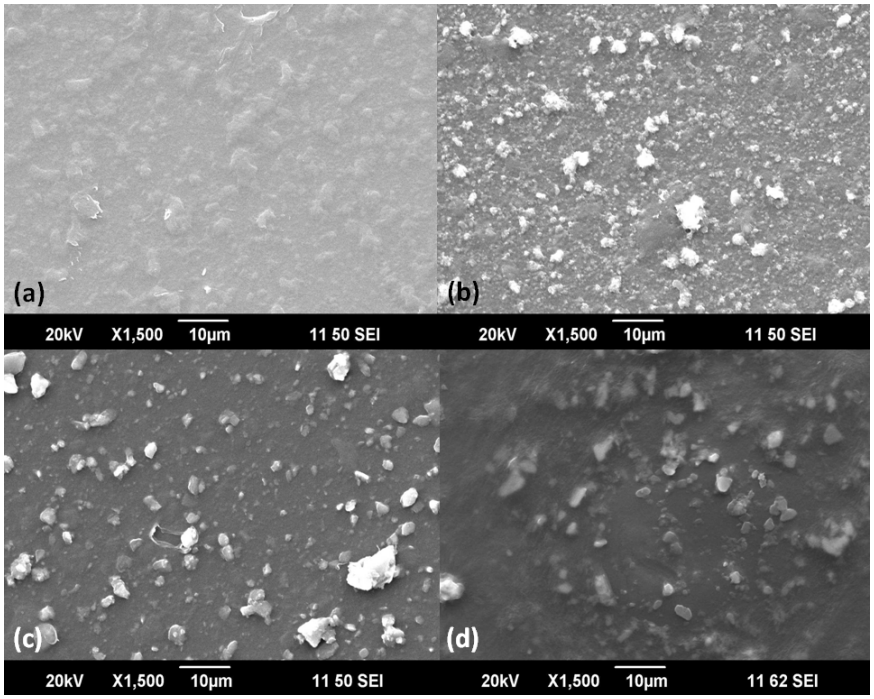

Figure 2. SEM images of the samples a) pristine P3HT film, b) P3HT:ZnS_{Cubic} film, c) P3HT:ZnS_{Hexa} film, d) P3HT:ZnS_{Hexa}:PVA-Ag.

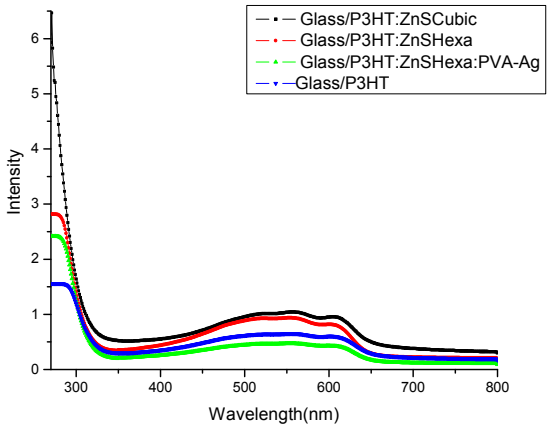

Figure 3. Optical absorption spectra of active materials.

Al, and it will not happen if the electron acceptor is buried inside the P3HT polymer matrix.

UV-Vis absorption measurements can show the absorption and transmission characteristics of these films and the absorption spectrum obtained by Varian, Cary 5000 Spectrophotometer. Figure 3 shows the absorption spectra of the P3HT: ZnS and P3HT: ZnS: PVA-Ag samples and it shows a broad absorption from 400nm to 650nm. Previous reports of P3HT also showed a broad absorption spectra from 320 to 650nm [7, 18, 19] and reported that it varies depending on the solvent but it is around 500nm. Absorption can be attributed to the p–p* transitions [7]. UV–Vis spectrum of blend shown in figure 3 is simply the combination of constituents parts of the active materials i.e. nanocrystals and polymer without any additional absorption peaks [7, 18, 19] since there isn't any ground state interactions between them levels when adding [20]. It is seen that the absorption spectra of the ZnS:P3HT blend is little extended to the lower nanoparticles decreases the inter-chain interaction and conjugation length of P3HT [7]. Remarkable finding here is that the addition of the ZnS in to P3HT matrix increases the magnitude of absorption which can be attributed to the crystallization of the P3HT and is thus able to capture more incoming light [21, 22, 23].

P3HT:ZnS, P3HT:ZnS:PVA-Ag nano composites were further analyzed by Bruker AXS D8 Advance X-Ray Powder Diffractometer for finding their crystal information. Resulting x-ray diffractograms are shown in figure 4 and are compared with pristine P3HT also. Diffractogram of pristine P3HT and other samples also shows diffraction peak at around 5.5° that corresponds to P3HT and the results of Yun et al. (on P3HT:TiO_2) [18], Greene et al. (on P3HT:ZnO) [24] and Zhokhavets et al. [21] (in them the peak was between 5 and 6) . But Dong et al. [19] shows that the amorphous P3HT has peak only at around 21.81. It is evident from our four samples and from other previous three results [18, 24, 21] that the peak of P3HT is around 5.5°. Other peaks observed in the resulting x-ray diffractograms are due to the presence of ZnS and PVA. Other crystal information obtained from the diffractograms is tabulated in table 2**.**

Diffraction peak of P3HT was observed due to the annealing of the sample, since annealing improves the crystallinity of P3HT [24]. Further, the crystalline nature of P3HT improves the hole mobility and the peak around 5° is due to (100) planes that is originated from crystals with their alkyl chains oriented from perpendicular and their pi-pi stacking axis parallel to the substrate surface [21]. Zhokhavets et al. [21] reports the interplanar spacing of the polymer crystallites as 1.68 nm and the diffraction peak is due to a-axis orientation. Also the backbone of the polymer is parallel and side-chains are perpendicular to the substrate having lattice constants b and c as 0.383 nm and0.385 nm, respectively [21,25].

Current voltage (I-V) measurements are basically a

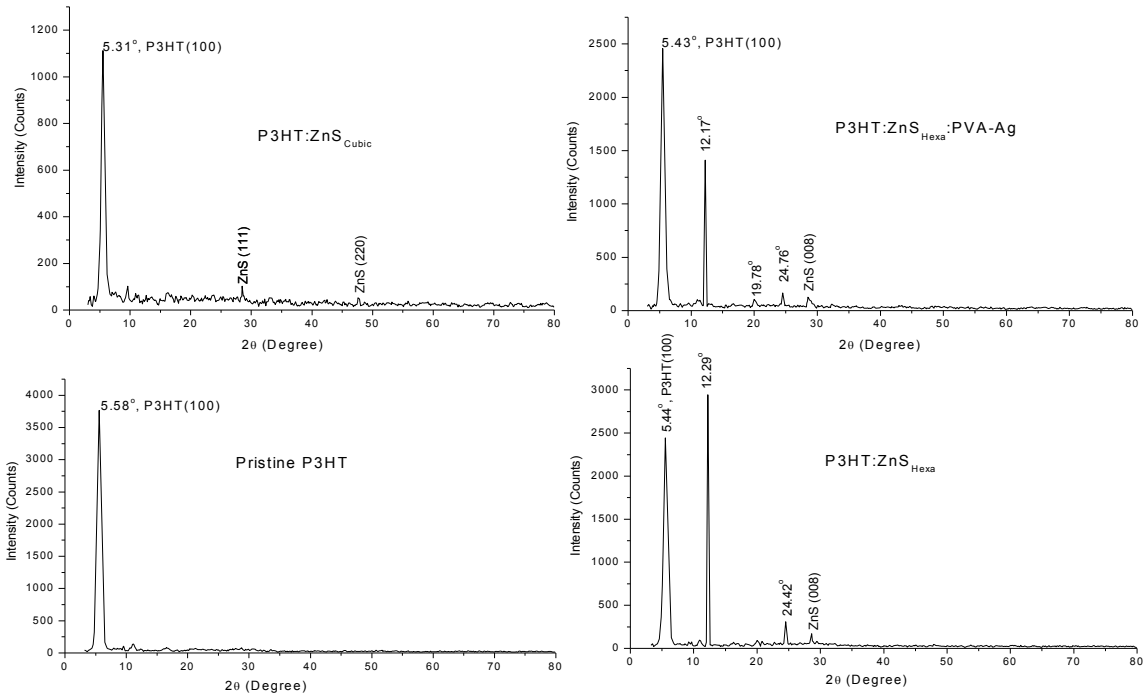

Figure 4. X-ray diffractogram of the samples.

Table 2. Crystal information of P3HT and P3HT: ZnS samples.

Sample Name	2 θ (Degree)	Interplanar spacing (d) nm	Standard Values (nm)	Crystal Planes
P3HT	5.58	1.5835	1.68[56]	(100)
P3HT:ZnS_{Cubic}	5.31	1.6629	1.68[56]	(100)
	28.549	0.3124	0.3126(ASTM:77-2100)	(111)
	47.51	0.1912	0.1914(ASTM:77-2100)	(220)
P3HT:ZnS_{Hexa}	5.44	1.6232	1.68[56]	(100)
	12.29	0.7196	PVA [153]	
	24.42	0.3642	PVA[153]	
	28.59	0.3119	0.3120(ASTM:39-1363)	(008)
P3HT:ZnS_{Hexa}:PVA-Ag	5.43	1.6262	1.68[56]	(100)
	12.17	0.7267	PVA[153]	
	19.78	0.4485	PVA [154,155]	
	24.76	0.3593	PVA[153]	
	28.55	0.3124	0.3120(ASTM:39-1363)	(008)

simple process and the results can be interpreted in a variety of ways to obtain a number of useful parameters. Current-voltage (I-V) measurements were obtained in dark using a two probe arrangement (DC Probe Station 1 at CEN, IISc. Bangalore) and the data can be used to calculate the density of state at Fermi level, activation energy, hopping distance, hopping energy, Mott's characteristic temperature and conductivity of component materials of hybrid organic solar cells.

In order to determine the current conduction mechanism in P3HT, P3HT:ZnS and P3HT:ZnS:PVA-Ag composite films, the temperature dependence of electrical conductivity was studied in the temperature range from 303 K, 323K and 353K. The electrical conductivity behavior of the hybrid organic samples can be explained using two different models: a) Arrhenius Model and b) Variable Range Hopping Model.

3.1. Arrhenius model

Logarithmic plot of DC conductivity as a function of reciprocal temperature is shown in figure 5. This type of electrical conductivity behavior follows Arrhenius model

Table 3. Activation energy and conductivity from Arrhenius plot.

Sample	Slope	σ_0 S/m	R^2	Eg(eV)	Conductivity (σ) S/m
P3HT	-8.3453	16.7981	0.9192	0.7189	3.4127
P3HT:ZnS_{Cubic}	-5.9830	8.9380	0.9677	0.5154	3.0876
P3HT:ZnS_{Hexa}	-7.7910	12.8904	0.8060	0.6711	3.3413
P3HT:ZnS_{Hexa}:PVA-Ag	-10.3868	19.4134	0.9211	0.8947	3.6170

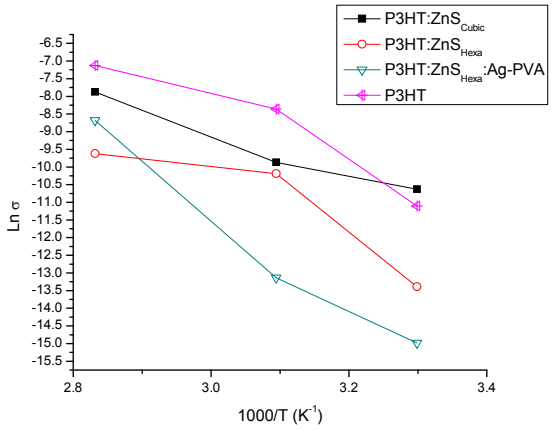

Figure 5. Logarithmic *dc* conductivity vs. 1000/T.

[26] and according to this model conductivity and temperature can be related as

$$\sigma = \sigma_0 \exp\left[\frac{-E_a}{kT}\right], \quad (1)$$

where σ_0 is the pre-exponential factor constant, k is the Boltzmann constant (8.617 3×10^{-5} eV/K) and E_a is the carrier activation energy. It is deduced from the graph that conductivity exhibits a thermally activated process in the measured temperature range. The slope of this curve is found from the best linear fit using Origin 7.5 software, since the slope gives the activation energy (slope = - E_a / 1000k) and the data are tabulated with the goodness of the fit (R^2) in table 3. The present activation energy is consistent with previous reported thermal activation energy of P3HT (~0.8 eV) [27-29] and this is related to the trap depth of the device where charge carriers are activated by thermal energy from traps, and are hopped to the nearest site [27,28,30,31]. It is deduced that room temperature DC conductivity of the pristine P3HT is 3.4127 S/m and conductivity variation is negligible even when ZnS particles are dispersed with P3HT.

3.2. Variable range hopping model

Since disorder plays an important role in conducting polymers, Variable Range Hopping (VRH) is also considered as one of the major carrier transport mechanisms, which is originally proposed for inorganic amorphous semiconductors. Hopping refers to tunneling transitions from occupied to unoccupied localized states and is based upon the assumption that energy difference is maintained by emission or absorption of one or more phonons. Temperature dependence of conductivity in organic semiconductors is described by Mott's VRH mechanism which includes the phonon assisted quantum mechanical transport phenomenon for the movement of charge carriers and hopping distance is not constant in this type of conduction. According to this model, the characteristic temperature dependence of conductivity [32] is given by

$$\sigma = \sigma_0 \exp\left[\frac{-T_o}{T}\right]^{\gamma}, \quad (2)$$

$$\gamma = \frac{1}{(1+d)}, \quad (3)$$

where σ_0 is high temperature limit of conductivity, T_o is Mott's characteristic temperature associated with degree of localization of electronic wave function, exponent determines the hopping space dimensionality of the charge transport in conducting medium, d is the dimensionality factor and the values 3, 2 and 1 are for three, two and one dimensional hopping transport respectively.

In order to evaluate the possibility of *VRH* and dimensionality of conduction process in polymeric films, semi logarithmic plot of conductivity as a function of $(1/T)^{1/4}$ or $(1/T)^{1/3}$ or $(1/T)^{1/2}$ is drawn to get a straight line according to eq. (2), experimental and the values of the prepared films conductivity have been plotted in figures 6. Best fit values are found from linear regression using Origin 7.5 Software and tabled in table 4. It is evident from the Mott VRH plots that Mott's law is obeyed over the temperature range from 303 K to 353K and indicates 3-D charge transport in P3HT:ZnS_{Cubic}, 2-D transport in P3HT:ZnS_{Hexa}:PVA-Ag and 1-D transport in P3HT:ZnS_{Hexa} and in pristine P3HT samples. So that the hopping parameters can be found from [33,34]

$$T_o = \frac{18}{r_o^3 kN(E_F)}, \quad (4)$$

where r_o is the localization length, k is the Boltzmann constant and $N(E_F)$ is the density of state at Fermi level. It is assumed here that the electron wave function localization length (r_o) is equal to the width of thiophene monomer unit, since the electrons are always at least delocalized to the extent of π-orbitals on the monomer units, which is about 3.185 Å [31]. The values of Mott's characteristic temperature T_o can be found from the slope of $ln\sigma$ vs $T^{-\gamma}$. Further, hopping distance (R) and average hopping energy (W) can be found from the Mott and Davis relation [33]

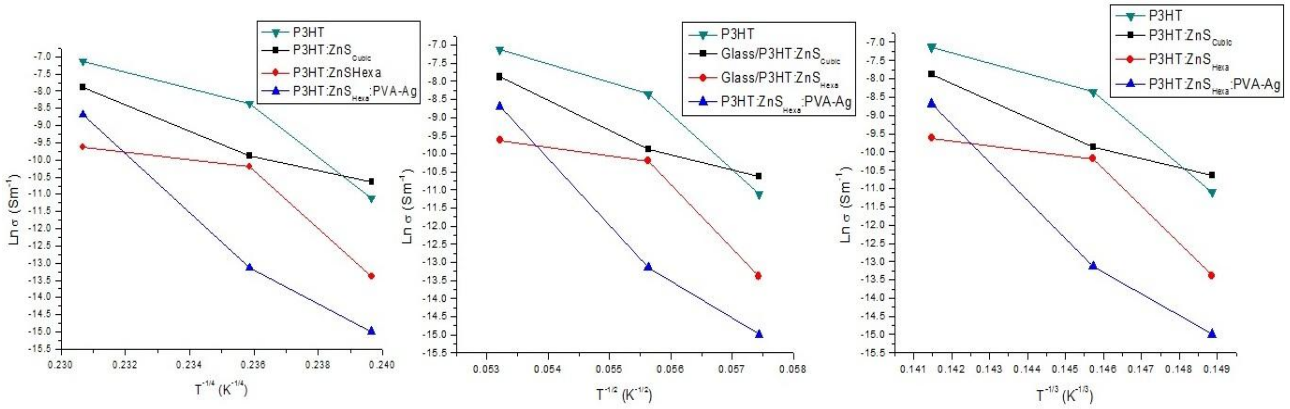

Figure 6. a) Lnσ vs. $T^{-1/4}$ graph. b) Lnσ vs. $T^{-1/2}$ graph. c) Lnσ vs. $T^{-1/3}$ graph.

Table 4 Variable Range Hopping data of the sample

Samples	R^2	Slope	T_o K (10^{10})	Intercept ($ln\sigma_o$)	σ_o S/m	N(Ef) m^{-3} eV^{-1} (10^{22})	R Å	W eV	R/ro
P3HT	0.9103	-431.62	3.4706	92.7386	$1.89x10^{40}$	1.7164	224.636	1.2276	70.5294
P3HT:ZnS_{Cubic}	0.9732	-311.833	0.9456	63.9450	$5.90x10^{27}$	6.2999	162.293	0.8869	50.9545
P3HT:ZnS_{Hexa}	0.7926	-401.716	2.6042	83.4958	$1.83x10^{36}$	2.2874	209.073	1.1426	65.643
P3HT:ZnS_{Hexa}:PVA-Ag	0.9124	-522.612	7.4596	110.4793	$9.56x10^{47}$	0.7986	271.992	1.4865	85.3978

$$R = \left[\frac{9r_o}{8\pi kTN(E_F)}\right]^{\frac{1}{4}}, \quad (5)$$

and

$$W = \frac{3}{4\pi R^3 N(E_F)}. \quad (6)$$

The condition for VRH conduction process is $R/r_o >> 1$ and $W >> kT$. Average hopping energy is decreased in the case of ZnS added P3HT less than pristine P3HT, where little energy is required by carrier to make a transition between two states in hopping process but it is seen that the disorder is increased in the case of PVA-Ag added ZnS:P3HT system, since more energy is needed to make a transition than in pristine P3HT.

4. Conclusion

Optical, structural and conduction mechanism of P3HT:ZnS nanocomposites were studied and the conduction mechanism was explained by Arrhenius model and variable range hopping method. It is found from both methods that little energy is required to make a transition between two states in hopping process in the case of ZnS added P3HT, but the disorder was increased when PVA coated silver nanoparticles was added to ZnS:P3HT. Further, the addition of semiconductor nanoparticles does not make any remarkable change in room temperature DC conduction of P3HT polymer but their absorption is increased.

Acknowledgement

The authors acknowledge Dr. Praveen C. Ramamurthy, Arun D. Rao (Department of materials engineering, IISc, Bangalore), INUP, CEN @ IISc., Bangalore and Sophisticated Test and Instrumentation Centre, CUSAT, Cochin, Kerala for completing this work.

References

1. D I Black, "*Fabrication Of Hybrid Inorganic And Organic Photovoltaic Cells*", PhD thesis, Emerging Technologies Research Centre, De Montfort University, Leicester, London (2011).
2. H E Unalan, P Hiralal, D Kuo, B Parekh, G Amaratunga, and M Chhowalla, *J. Mater. Chem.* **18** (2008) 5909.
3. J U Lee, J W Jung, T Emrick, T P Russell , and W H Jo , *J. Mater. Chem.* **20** (2010) 3287.
4. G K Mor, K Shankar, M Paulose, O K Varghese, and C A Grimes, *Appl. Phys. Lett.* **91** (2007) 152111.
5. J H Lee, J H Park, J S Kim, D Y Lee, and K Cho, *Organic Electronics* **10** (2009) 416.
6. M Bredol, K Matras, A Szatkowski, J Sanetra, and A P Schwa, *Sol. Mat. Sol. C.* **93** (2009) 662.
7. M Mall, P Kumar, S Chand, and L Kumar, *Chem. Phys. Lett.* **495** (2010) 236.
8. B R Saunders and M L Turner, *Adv. Colloid Interfac.* **138**,1 (2008) 1.
9. A Kongkanand, K Tvrdy, K Takechi, M Kuno, and P V Kamat, *J. Am. Chem. Soc.* **130**, 12 (2008) 4007.
10. W Martienssen and H Warlimont, "*Springer Handbook of Condensed Matter and Materials Data*" ed. 1, Springer, New York (2005).
11. Y Yang, S Xue, S Liu, J Huang, and J Shen, *Appl. Phys. Lett.* **69** (1996) 377.
12. T Abdul kareem and A Anu kaliani, *Arabian Journal of Chemistry* **4** (2011) 325.
13. H Y Chen, M K F Lo, G Yang, H G Monbouquette, and Y Yang, *Nature Nanotechnology* **3** (2008) 543.
14. Y Ding , P Lu, and Q Chen, *Proc. of SPIE* Vol. **7099** (2008) 709919.

15. Y T Chang, S O L Hsu, M H Su, and K H Wei, *Adv. Mater.* **21** (2009) 2093.
16. Y Kim, S A Choulis, J Nelson J, D D C Bradley, S Cook, and J R Durrant, *Appl. Phys. Lett.* **86** (2005) 063502.
17. J Lee, A Kim, S M Cho, and H Chae, *Korean J. Chem. Eng.* **29**, 3 (2012) 337.
18. T W Yun and K Sulaiman, *Sains Malaysiana* **40**, 1 (2011) 43.
19. Z Hu, T Daeri, M S Bonner, and A J Gesquiere, *J. Lumin.* **130,** 5 (2010) 771.
20. Y Dong, J Lu, F Yan, and Q Xu, *High Perform. Polym.* **21** (2009) 48.
21. U Zhokhavets, T Erb, H Hoppe, G Gobsch, and N S Sariciftci, *Thin Solid Films* **496** (2006) 679.
22. J Guo, H Ohkita, H Benten, and S Ito, *J. Am. Chem. Soc.***132** (2010) 6154.
23. W H Lee, S Y Chuang, H L Chen, W F Su, and C H Lin, *Thin Solid Films* **518** (2010) 7450.
24. L E Greene, M Law, B D Yuhas, and P Yang, *J. Phys. Chem. C* **111**, 50 (2007) 18451.
25. J U Lee , J W Jung, T Emrick, T P Russell, and W H Jo, *Nanotechnology* **21**(2010) 105201.
26. M Khissi, M E Hasnaoui, J Belattar, M P F Graça, M E Achour, and L C Costa, *J. Mater. Environ. Sci.* **2**, 3 (2011) 281.
27. D Choi, S Jin, Y Lee, S H Kim, D S Chung, K Hong, C Yang, J Jung, J K Kim, M Ree, and C E Park, *Appl. Mater. Interfaces*, **2**, 1 (2010) 48.
28. J C Nolasco, R Cabré, J Ferré-Borrull, L F Marsal, M Estrada, and J Pallarès, *J. Appl. Phys.***107** (2010) 044505.
29. J A Letizia, J Rivnay, A Facchetti, M A Ratner , and T J Marks, *Adv. Funct. Mater.* **20** (2010) 50.
30. Y Park, S Noh, D Lee, J Y Kim and C Lee C., *J. Korean Phys. Soc.* **59**, 2 (2011) 362.
31. R K Singh, J Kumar, R Singh, R Kant, R C Rastogi, S Chand, and V Kumar, *New J. Phys.* **8** (2006) 112.
32. N Othman, Z A Talib, A Kassim, A H Shaari, and J Y C Liew, *Journal of Fundamental Sciences* **5** (2009) 29.
33. A A Hendi, *Life Sci. J.* **8** (2011) 3.
34. M Taunk, A Kapil and S Chand, *The Open Macromolecules Journal* **2** (2008) 74.